

Supporting Information

***In Situ Growth and Pyrolysis Synthesis of Super-hydrophobic
Graphene Aerogels Embedded with Ultrafine β -Co Nanocrystals for
Microwave Absorption***

Dongwei Xu^a, Jialiang Liu^a, Ping Chen^{a,*}, Qi Yu^{b,*}, Jing Wang^b, Sen Yang^a, Xiang Guo^a

^a. State Key Laboratory of Fine Chemicals, Dalian University of Technology, Dalian (116024), China

E-Mail: chenping_898@126.com

^b. Liaoning Key laboratory of advanced polymer matrix composites, Shenyang Aerospace University,

Shenyang (110136), China

E-Mail: yuqi1027@126.com

Fig. S1 Typical digital photograph of (a) GO suspension, (b) macroscopic photographs of rGO/AACo/PVA hydrogel.

Fig. S2 XRD patterns of graphite and the as-synthesized sample of GO.

Fig. S3 SEM/EDS elemental mapping images of (b) C, (c) O and (d) Co.

Fig. S4 (a) Water contact angle of SMGA-Co at calcination temperature of 700 °C.

(b) Water contact angles of SMGA-Co at different calcination temperatures.

Fig. S5 C 1s XPS spectra of SMGA-Co at different annealing temperatures:(a) 400°C,(b) 500°C, (c) 600°C,(d) 550°C.

Fig. S6 Water droplet sliding on a homemade U-shaped trajectory, which is fabricated by anchoring the SMGA-Co nanocomposites on a flexible aluminum substrate.

Fig. S7 Reflection loss values of SMGA-Co at different thicknesses.

Table S1 Computation of atom ratio for Graphite, GO, GA and SMGA-Co.

Table S2 Typical Co-based and graphene-based composites for MA performance in open literatures.

Table S3 The conductivity and resistivity of different samples

Supplementary Notes: impedance matching ratio (Z) and attenuation constant (α).

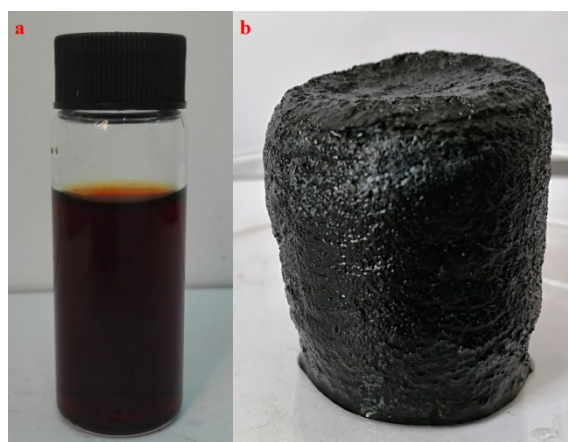


Fig. S1 Typical digital photograph of (a) GO suspension, (b) macroscopic photographs of rGO/AACo/PVA hydrogel

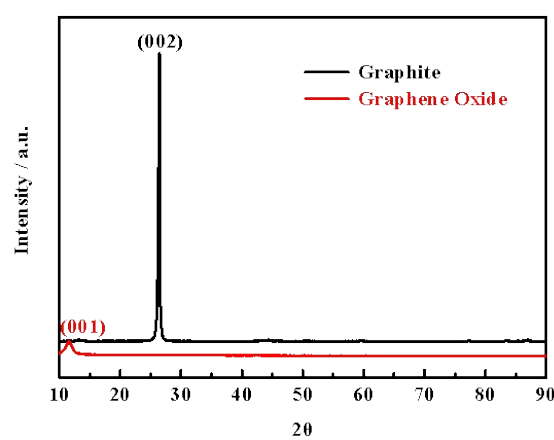


Fig. S2 XRD patterns of graphite and the as-synthesized sample of GO.

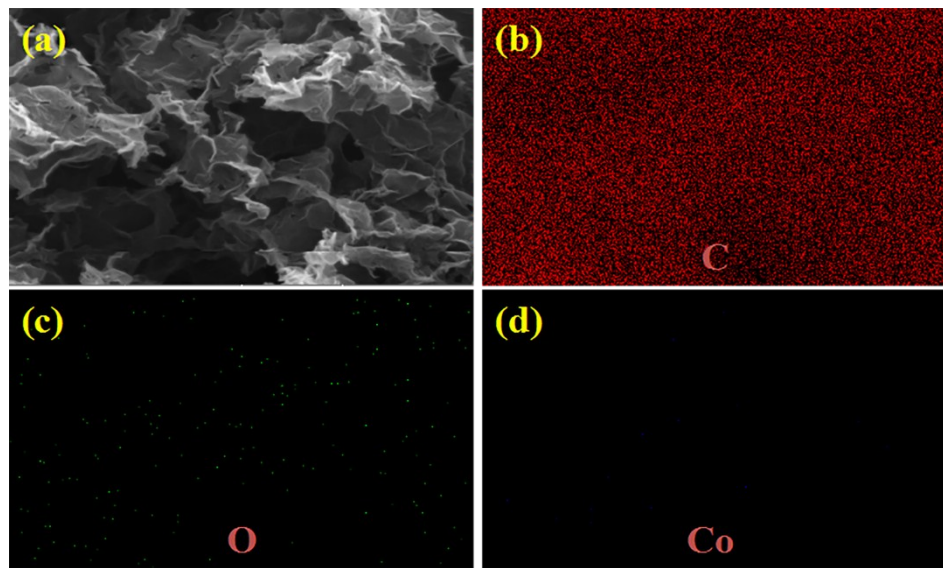


Fig. S3 SEM/EDS elemental mapping images of (b) C, (c) O and (d) Co.

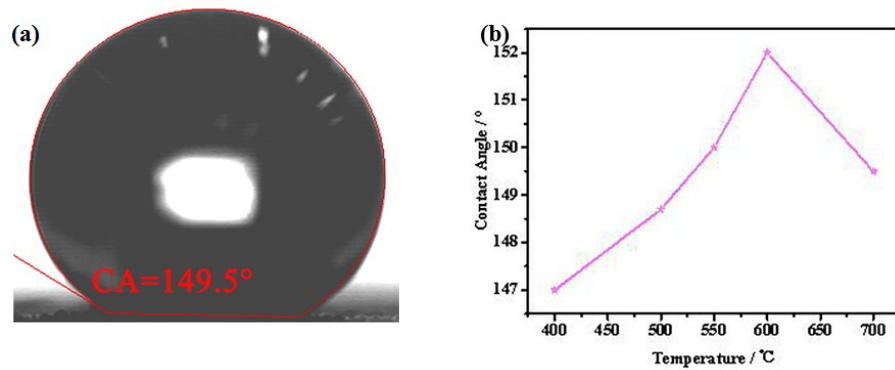


Fig. S4 (a) Water contact angle of SMGA-Co at calcination temperature of $700\text{ }^\circ\text{C}$.

(b) Water contact angles of SMGA-Co at different calcination temperatures.

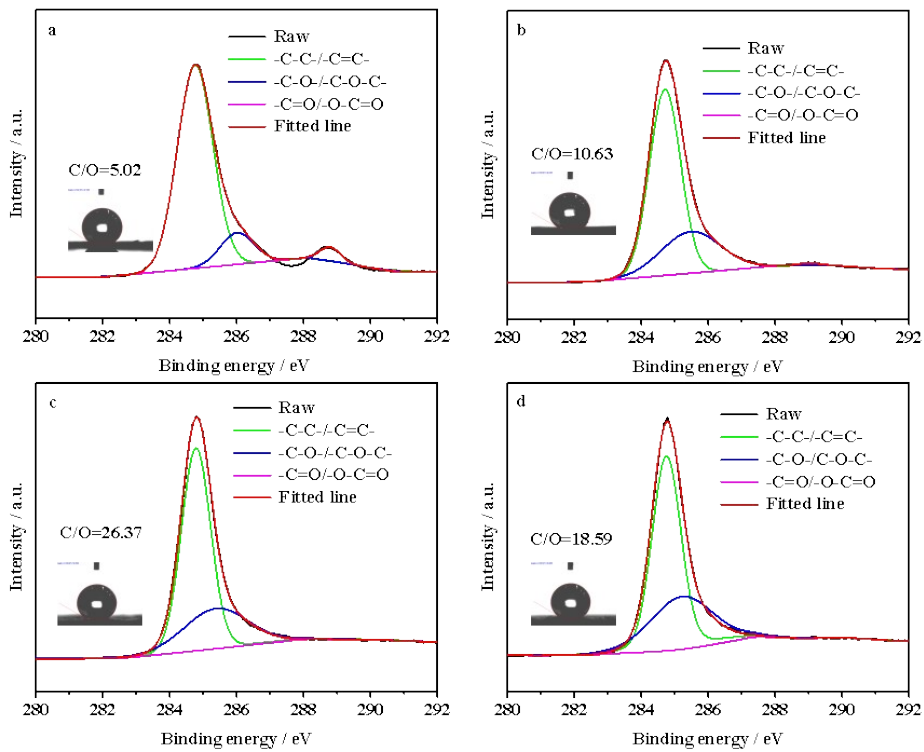


Fig. S5 C 1s XPS spectra of SMGA-Co at different annealing temperatures:(a) 400°C,(b) 500°C, (c) 600°C,(d) 550°C.

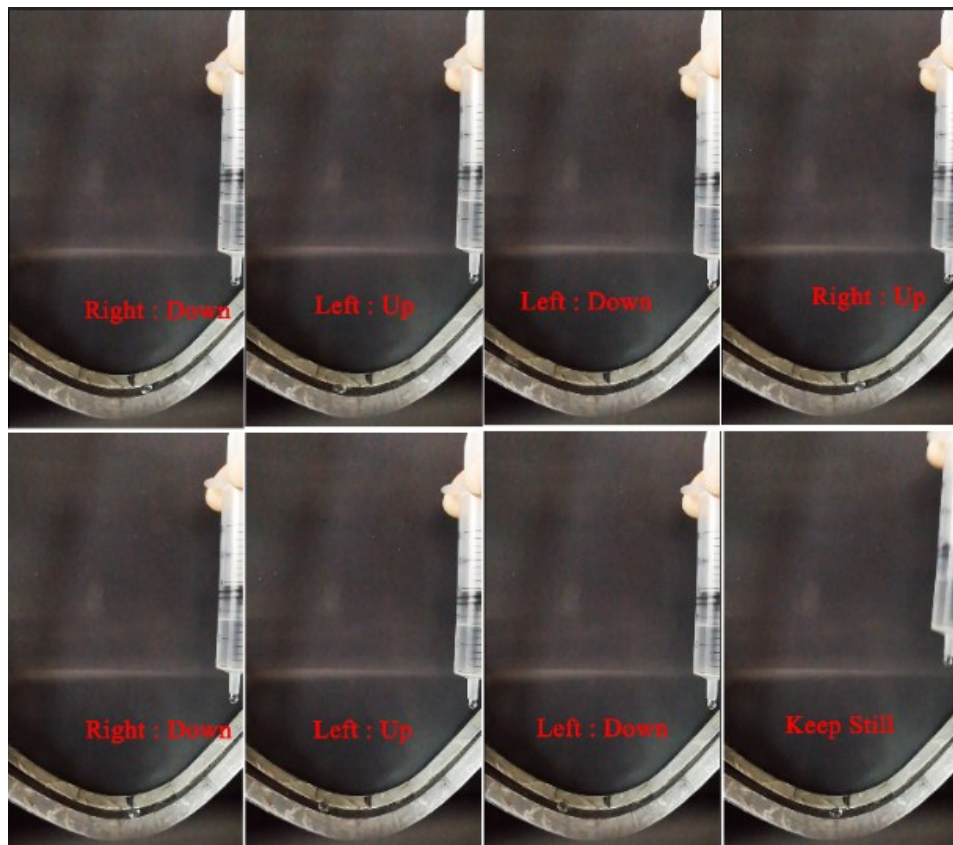


Fig. S6 Water droplet sliding on a homemade U-shaped trajectory, which is fabricated by anchoring the SMGA-Co nanocomposites on a flexible aluminum substrate.

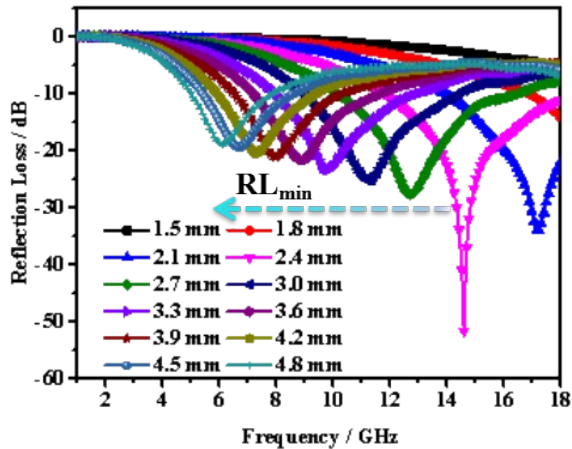


Fig. S7 Reflection loss values of SMGA-Co at different thicknesses.

Table S1 Computation of atom ratio for Graphite, GO, GA and SMGA-Co.

	I _D /I _G	C/O (at.%)
Graphite	0.76	---
GO	1.38	72.9/27.1 (2.69)
SMGA-Co	1.79	94.44/5.08 (18.59)
GA	1.85	95.12/4.88 (19.49)

Table S2: Typical Co-based and graphene-based composites for MA performance in open literatures

Samples in matrices	wt %	Max RL [dB]	Thickness [mm] (RL ≤ -10 dB)	Testing frequency [GHz]	Frequency range [GHz] (RL ≤ -10 dB)	Refs
SMGA-Co composites in paraffin	4.25	-51.6	2.4	1-18	11.5-18	This work
Co/CNT/Graphene	30	-65.6	2.19	2-18	10-13	[1]
Co/GN nanocomposites	60	-47.5	2.0	1-18	-----	[2]
Co@CoO	50	-90.2	1.3	2-18	12-15.5	[3]
Co/C	30	-40	5.0	2-18	-----	[4]
Co dendrites	65	-35.6	3.0	1-18	10.5-14.5	[5]
Co-CoO composites	60	-30.5	1.7	2-18	12.6-17.3	[6]
Co _x Fe _{3-x} O ₄ spheres	75	-41	2.0	2-18	X band	[7]
CoFe ₂ O ₄ hollow sphere/graphene	60	-18.5	2.0	1-18	11.3-15	[8]
Porous Fe ₃ O ₄ -decorated graphene	30	-44.2	3.0	0.5-18	4.1-6.8	[9]
RGO-Fe ₃ O ₄	40	-15.4	2.0	0.5-18	10.4-13.2	[10]
GO/CNT-Fe ₃ O ₄	30	-37.3	5	2-18	<1	[11]
Ni-graphene	20	-13	2.0	2-18	9.6-12.2	[12]
Thermally reduced graphene	1	-43.5	3.5	2-18	9.4-16.8	[13]
graphene/SiO ₂	7	-42	2.1	X-band	8.4-12	[14]
3D Graphene-Ni	33	-59.7	2.7	1-18	9.4-14.2	[15]
rGO/a-Fe ₂ O ₃ composite	8	-33.5	3.0	1-18	10.8-17.2	[16]
Fe ₃ O ₄ /GCs Composites	30	-32	3.5	2-18	6.9-11.9	[17]

Table S3 The conductivity and resistivity of different samples

sample	Graphene oxide	graphene	Graphene aerogels	SMGA-Co
σ (S/m)	0.0150	0.0880	0.0145	0.0731
ρ ($\Omega \cdot m$)	66.7	11.4	69.0	13.7

Supplementary Notes

Supplementary Note S1: the integral area (ΔS) and the microwave absorption efficiency (R_E)

Maximum reflection loss (RL) and effective absorption bandwidth (EAB) are two parameters to assess the microwave absorption properties. The corresponding thicknesses are not consistent, however, the data are not comparable. Hence, it is difficult to judge which thickness is the appropriate absorber thickness to obtain the best microwave absorption properties. Thus, we use the integral area (ΔS when RL value is below -10 dB) to determine microwave absorption performance. We define ΔS as equal to the integral area when $RL < -10$ dB. Then the microwave absorption efficiency (R_E) is defined as $R_E = \Delta S / d$.

Supplementary Note S2: Basic concepts of impedance matching ratio (Z) and attenuation constant (α).

The enhanced microwave absorption properties mainly resulted from the impedance matching Z and attenuation constant α , as expressed by the following equation:

$$\alpha = \frac{\sqrt{2\pi f}}{c} \times \sqrt{(\mu''\epsilon'' - \mu'\epsilon') + \sqrt{(\mu''\epsilon'' - \mu'\epsilon')^2 + (\mu'\epsilon'' - \mu''\epsilon')^2}} \quad (1)$$

$$Z = \sqrt{\sqrt{(\mu'^2 + \mu''^2)} / \sqrt{(\epsilon'^2 + \epsilon''^2)}} \quad (2)$$

Where f and c are the frequency of the electromagnetic wave and the velocity of light, respectively.

The incident electromagnetic wave irradiates on the surface of the materials from free space, reflection and transmission phenomena will happen at the interfaces. In order to realize the efficient absorption of electromagnetic waves, it is important to make electromagnetic waves through the material surface as much as possible. Then, the absorption materials could effectively attenuate electromagnetic waves by converting them into thermal energy or dissipating them through interference. The impedance match requires that the relation between permittivity and permeability tends to be close, which can achieve zero-reflection at the front surface of the materials.

REFERENCES

1. Qi, X. S.; Hu, Q.; Xu, J. L.; Xie, R.; Jiang, Y.; Zhong, W.; Du, Y. W. The Synthesis and Excellent Electromagnetic Radiation Absorption Properties of Core/Shell Structured Co/Carbon Nanotube-Graphene Nanocomposites. *RSC Adv.* **2016**, 6, 11382-11387.
2. Pan, G. H.; Zhu, J.; Ma, S. L.; Sun, G. B.; Yang, X. J. Enhancing the Electromagnetic Performance of Co through the Phase-Controlled Synthesis of Hexagonal and Cubic Co Nanocrystals Grown on Graphene. *ACS Appl. Mater. Interfaces* **2013**, 5, 12716-12724.
3. Liu, T.; Pang, Y.; Zhu, M.; Kobayashi, S. Microporous Co@CoO Nanoparticles with Superior Microwave Absorption Properties. *Nanoscale* **2014**, 6, 2447-2454.
4. Liu, Q. L.; Zhang, D.; Fan, T. X. Electromagnetic Wave Absorption Properties of Porous Carbon/Co Nanocomposites. *Appl. Phys. Lett.* **2008**, 93, 013110.
5. Wang, X. L.; Shi, G. M.; Shi, F. N.; Xu, G.; Qi, Y. Y.; Li, D.; Zhang, Z. D.; Zhang, Y. J.; You, H. P. Synthesis of Hierarchical Cobalt Dendrites Based on Nanoflake Self-Assembly and Their Microwave Absorption Properties. *RSC Adv.* **2016**, 6, 40844-40853.
6. Wang, Z. Z.; Bi, H.; Wang, P. H.; Wang, M.; Liu, Z. W.; Shen, L.; Liu, X. S. Magnetic and Microwave Absorption Properties of Self-Assemblies Composed of Core-Shell Cobalt-Cobalt Oxide Nanocrystals. *Phys. Chem. Chem. Phys.* **2015**, 17, 3796-3801.
7. Ji, R. L.; Cao, C. B.; Chen, Z.; Zhai, H. Z.; Bai, J. Solvothermal Synthesis of $\text{Co}_x\text{Fe}_{3-x}\text{O}_4$ Spheres and Their Microwave Absorption Properties. *J. Mater. Chem. C* **2014**, DOI: 10.1039/c4tc00167b.
8. Fu, M.; Jiao, Q. Z.; Zhao, Y.; Li, H. S. Vapor Diffusion Synthesis of CoFe_2O_4 Hollow Sphere/Graphene Composites as Absorbing Materials. *J. Mater. Chem. A* **2014**, 2, 735-744.
9. Sun, D. P.; Zou, Q.; Qian, G. Q.; Sun, C.; Jiang, W.; Li, F. S. Controlled Synthesis

- of Porous Fe₃O₄-Decorated Graphene with Extraordinary Electromagnetic Wave Absorption Properties. *Acta Mater.* **2013**, 61, 5829-5834.
10. Sun, X.; He, J. P.; Li, G. X.; Tang, J.; Wang, T.; Guo, Y. X.; Xue, H. R. Laminated Magnetic Graphene with Enhanced Electromagnetic Wave Absorption Properties. *J. Mater. Chem. C* **2013**, 1, 765-777.
11. Wang, L. N.; Jia, X. L.; Li, Y. F.; Yang, F.; Zhang, L. Q.; Liu, L. P.; Ren, X.; Yang, H.T. Synthesis and Microwave Absorption Property of Flexible Magnetic Film Based on Graphene Oxide/Carbon Nanotubes and Fe₃O₄ Nanoparticles. *J. Mater. Chem. A* **2014**, 2, 14940-14946.
12. Cao, Y.; Su, Q.; Che, R.; Du. G.; Xu, B. One-Step Chemical Vapor Synthesis of Ni/Graphene Nanocomposites with Excellent Electromagnetic and Electrocatalytic Properties. *Synth. Met.* **2012**, 162, 968-973.
13. Liu, W. W.; Li, H.; Zeng, Q. P.; Duan, H. N.; Cuo, Y. P.; Liu,X. F.; Sun, C. Y.; Liu, H. Z. Fabrication of Ultralight Three-Dimensional Graphene Networks with Strong Electromagnetic Wave Absorption Properties, *J. Mater. Chem. A* **2015**, 3, 3739-3747.
14. Cao, W. Q.; Wang, X. X.; Yuan, J.; Wang, W. Z.; Cao, M. S. Temperature Dependent Microwave Absorption of Ultrathin Graphene Composites. *J. Mater. Chem. C* **2015**, 3, 10017-10022.
15. Zeng. Q. Xu. D. W., Chen. P., Yu. Q., Xiong. X. H., Chu. H. R., Wang. Q. 3D Graphene-Ni Microspheres with Excellent Microwave Absorption and Corrosion Resistance Properties. *J Mater Sci: Mater Electron.* **2018**, 29, 2421-2433.
16. Zhang, H.; Xie, A. J.; Wang, C. P.; Wang, H. S.; Shen, Y. H.; Tian, X. Y. Novel rGO/a-Fe₂O₃ Composite Hydrogel: Synthesis, Characterization and High Performance of Electromagnetic Wave Absorption. *J. Mater. Chem. A* **2013**, 1, 8547-8552.
17. Jian, X.; Wu, B.; Wei, Y. F.; Dou, S. X.; Wang, X. L.; He, W. D.; Mahmood, N.

Facile Synthesis of Fe₃O₄/GCs Composites and Their Enhanced Microwave Absorption Properties. *ACS Appl. Mater. Interfaces* **2016**, 8, 6101-6109.